Piezo-tuned nonplanar ring oscillator with GHz range and 100 kHz bandwidth

Thomas J. Kane*, Kenji Numata[a], Anthony Yu[a], Julia Majors[b] and David R. Demmer[b]
[a]NASA Goddard Space Flight Center, Greenbelt, MD, 20771 USA
[b]AVO Photonics, 120 Welsh Rd, Horsham, PA 19044 USA

ABSTRACT

We demonstrated a monolithic nonplanar ring oscillator (NPRO) with a piezo-electric tuning range of 3.5 GHz with 192 volts applied, corresponding to a tuning coefficient of 18.2 MHz/volt. Useful bandwidth was limited by a resonance at 338 kHz and an anti-resonance at 420 kHz. This performance was achieved by making the NPRO small, with a small distance between the piezo-electric transducer and the laser beam, and by using a piezo-electric material with favorable properties. This large frequency modulation range and wide frequency modulation bandwidth, combined with unsurpassed coherence and high power, make this an attractive laser for frequency-modulated continuous-wave (FMCW) LIDAR. The tested laser provides over 500 mW at 1064 nm. Comparable performance will be possible at the eye-safe Nd:YAG wavelength of 1319 nm.

Keywords: Frequency-tuned laser, FMCW LIDAR, nonplanar ring oscillator

1. INTRODUCTION

The nonplanar ring oscillator, invented by Kane and Byer in 1984[1], sets the standard for narrow-linewidth single-frequency lasers. Single-frequency output at the several-hundred milliwatt level is commercially available at the two Nd:YAG wavelengths of 1064 nm and 1319 nm[2]. At 1064 nm, amplification can take power above 100 watts[3]. Lasers based on the NPRO design are critical elements in all laser interferometers used for gravitational wave detection[4].

The value of the NPRO is much enhanced by its convenient tunability. Thermal tuning provides multi-GHz tuning range and one-second response time. Strain tuning, accomplished using a piezo-electric element bonded to one of the non-optical surfaces of the NPRO, was invented by Kane in 1988[5]. Strain tuning has a response time of about one microsecond and, as initially reported, a range of a few tens of megahertz. This is more than adequate to enable robust phase locking of NPROs[6].

NASA is designing an NPRO for use as the laser oscillator for the Laser Interferometer Space Antenna (LISA) project[7]. This project will use three satellites in solar orbit to detect gravitational waves at low frequencies inaccessible to ground-based gravitational wave detectors.

The NASA variant of the NPRO design is designated the "micro-NPRO" or μNPRO. The European Space Agency (ESA) is the lead organization for the LISA project, and they require a strain-tuning range of ±100 MHz with bandwidth of 100 kHz. Typical commercial NPROs have a strain tuning coefficient of 1 MHz/volt, so meeting the ESA specification would require ±100 volts.

For use in space, it is desirable to keep voltages low and to simplify design. One of the goals (though not requirements) of the μNPRO design was to achieve ±100 MHz of strain tuning without the use of high-voltage amplifiers. Standard operational-amplifiers typically provide ±12 volts, so the goal was ±100 MHz tuning with ±12 volts, implying a strain-tuning coefficient of 8.33 MHz/volt or larger.

* Tom.Kane@ieee.org (650) 796-3469 KaneOE.com

Presented at Photonics West, January 26, 2022

We report strain tuning of the µNPRO with a tuning coefficient of 18.2 MHz/volt and a bandwidth of >200 kHz. The improvements over previous designs are based on four changes.

1. We made the µNPRO small. If all proportions are maintained, then both the piezo-electric strain tuning coefficient and the bandwidth increase as the inverse of the dimensional scaling factor.
2. We used piezo-electric material with the largest strain tuning figure-of-merit, defined as the product of the piezoelectric charge constant d_{31} and the Young's modulus Y.
3. We made NPROs with the internal beam very near to the surface on which the piezo-electric element is bonded.
4. We made the PZT element as thin as practical.

This paper has four sections in addition to the introduction and conclusion. Section 2 provides an overview of the NASA µNPRO design. Section 3 provides some approximate ways to calculate the tuning coefficient of an NPRO. To our knowledge, this is the first published theoretical analysis of strain tuning in NPROs. Section 4 presents our experimental results. Section 5 proposes that a µNPRO could be an excellent laser for long-range, high-resolution FMCW LIDAR.

2. THE NASA µNPRO

Figure 1 shows a completed µNPRO package. The overall dimensions of the enclosure are 58 x 41 x 14 mm, not including the feet and connector. The output light is in a polarization-maintaining single-mode fiber. The fiber alignment and fixing are based on welding. There is no isolator needed in the µNPRO package, due to the fact that the µNPRO has immunity to small amounts of feedback. The fiber entrance face is angle-polished and anti-reflection coated, so feedback from the fiber facet is low. The µNPRO package contains two pump lasers which are polarization-combined. If the pumps were operated at rated power the µNPRO package would provide over 0.7 watts of fiber-coupled single-frequency output at 1064 nm. The requirements of the LISA project are much lower (~0.07 watts), resulting in very long projected lifetime. The overall system being designed by NASA includes an ytterbium-doped fiber amplifier (YDFA), so all the µNPRO needs to do is to provide enough power to thoroughly saturate the input stage of the YDFA.

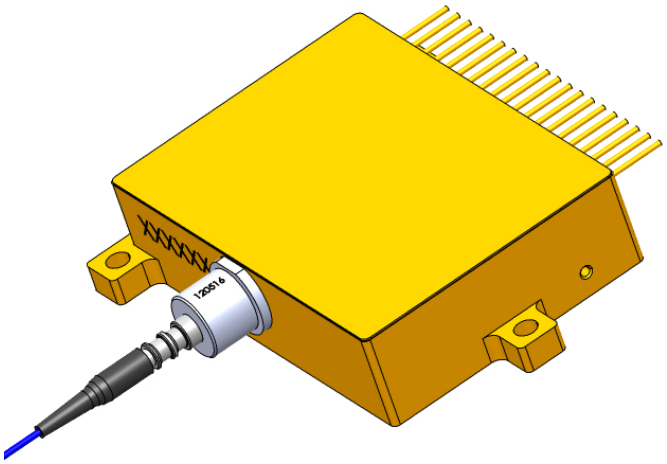

Figure 1. The µNPRO package. The overall dimensions of the enclosure are 58 x 41 x 14 mm, not including the feet. The output light is in a polarization-maintaining single-mode fiber.

Figure 2 shows the µNPRO crystal assembly. The view on the left side shows the µNPRO alone as a transparent object. The µNPROs are made of neodymium-doped yttrium aluminum garnet (YAG) co-doped with chromium. As with all NPROs, there are four optical facets, three of which are at angles to the overall block of YAG. The µNPRO has an out-of-plane angle of 45°. The overall dimensions of the µNPRO crystal are 5.7 x 4.4 x 1.75 mm.

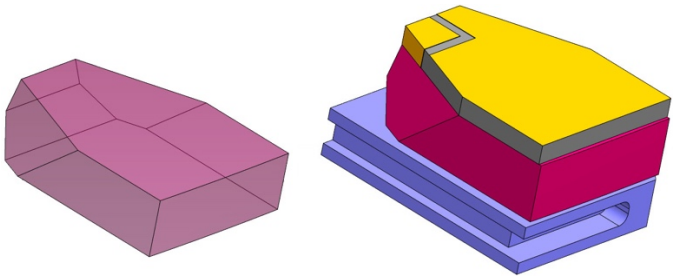

Figure 2. The μNPRO crystal. On left, the μNPRO, shown as a transparent object. On right, the μNPRO with the piezo-electric element attached on top and the temperature-controlled support structure shown below.

The view on the right shows the parts to which the μNPRO crystal are bonded. Below the μNPRO is a platform which is controlled in temperature by a thermo-electric cooler. Above the μNPRO is a piece of lead zirconium titanate (PZT.) This PZT element is bonded to the top surface of the μNPRO. The PZT is poled in its thin dimension so that when a voltage is applied to the PZT it attempts to reduce or increase the area of the bonded surface. This applies a strain to the μNPRO, which tunes the laser output.

3. THEORY OF STRAIN TUNING

In this section we will calculate the tuning coefficient in units of megahertz of optical frequency change per volt applied to the PZT element.

A full calculation would be quite an onerous task. Our goal is to provide design insight. So, in this section we carry out three simplified calculations that will give an idea of what it important and what is not.

When a laser is oscillating on a single mode and it is tuned by stretching the resonator by a small amount, the wavelength λ and optical frequency f change according to the equation

$$\frac{\Delta\lambda}{\lambda} = \frac{\Delta optical\ path\ length}{optical\ path\ length} = \frac{-\Delta f}{f}. \tag{1}$$

The fractional change in wavelength is the same as the fractional change in the optical path length of the resonator. This must be true since the same number of wavelengths fit into the resonator before and after the change in resonator length. For small changes, the fractional change in optical frequency is simply the negative of the fractional change in wavelength.

The change in optical path length is due to two effects. First is the simple dimensional change in the resonator, and second, the change in the index of refraction due to the elasto-optic effect. Initially, we ignore the elasto-optic effect. With this simplification, the fractional change in the optical path length is the same as the fractional change in dimension. The fractional change in dimension is by definition the mechanical strain, given by ϵ. Positive values of strain correspond to lengthening. The frequency change Δf is given by

$$\Delta f = -f\epsilon \tag{2}$$

where ϵ is the strain in the YAG crystal, averaged over the beam path.

Figure 3 shows the geometry of the PZT/YAG structure. A piece of PZT material is bonded to a piece of YAG. This PZT material is poled in the y direction, that is, the thin dimension of the PZT plate. The thickness of the PZT is t_{PZT} and the thickness of the YAG is t_{YAG}.

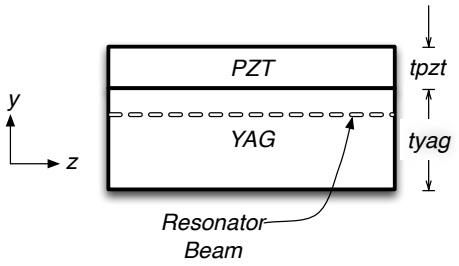

Figure 3. Diagram defining the dimensions and coordinates of the system.

3.1 Lumped element "two spring" model of strain

The first estimate of ϵ assumes that strain is uniform throughout the PZT/YAG structure. Under this assumption, the PZT and the YAG are considered as "lumped elements," specifically as simple springs. Each element is characterized by a spring constant. The two elements are connected in parallel in such a way that they must end up with the same length. Due to the voltage applied to the PZT, they would have slightly different lengths in their unconstrained state, if they were not bonded to each other. Each spring in the bonded state adjusts so that they end up with the same length, and with equal and opposite internal forces. Figure 4 shows this "parallel spring" model.

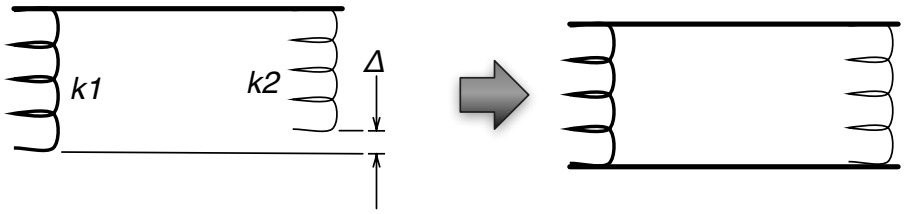

Figure 4. The simplest model of strain in the NPRO models the NPRO and the PZT as two springs of differing stiffness and length which are bonded together in parallel in such a way that they both deform to have the same length.

If two springs of spring constants k_1 and k_2 have a difference in their unconstrained lengths Δ, and they are tied together in such a way that they are forced to have the same length, then the change in the length of the spring with constant k_1 is given by

$$\Delta_1 = \frac{\Delta\, k_2}{k_1 + k_2} \tag{3}$$

The spring constant of each element in the PZT/YAG structure is proportional to $Y\,t\,/\,(1\text{-}\nu)$ where Y is the Young's modulus of the material, ν is Poisson's ratio, and t is the thickness of the element, either t_{PZT} or t_{YAG}. We will drop the Poisson's ratio divisor, since it will end up cluttering the final equation without much changing the result. It would show up only as the ratio $(1\text{-}\nu_{PZT})/(1\text{-}\nu_{YAG})$ and as can be seen by looking at Table 1, the Poisson's ratios of YAG and the PZT are similar. If you want to keep the effect of Poisson's ratio, simply replace Y by $Y/(1\text{-}\nu)$ in the equations for both materials.

When a voltage is applied to the PZT along the y dimension, and the PZT is unconstrained, the voltage-induced strain in both of the transverse dimensions x and z is given by

$$\epsilon_V = d_{31}\, E = d_{31}\, \frac{V}{t_{PZT}} \tag{4}$$

where d_{31} is a property of the PZT material and E is the electric field inside the PZT, equal to the applied voltage V divided by the thickness of the PZT t_{PZT}. This value ϵ_V plays the role of Δ, the difference in the unconstrained lengths of the two springs, that is, it is the amount by which the PZT would move relative to the YAG if they were not bonded together.

Carrying through the calculation using this spring analogy, the strain in the YAG is

$$\epsilon = \frac{V\, Y_{PZT}\, d_{31}}{(Y_{YAG} t_{YAG} + Y_{PZT} t_{PZT})}. \quad (5)$$

Combining this expression with Equation (2) and dividing out voltage V yields the tuning coefficient in units of Hertz per volt.

$$\textit{Tuning coefficient} = \frac{f\, Y_{PZT}\, d_{31}}{(Y_{YAG} t_{YAG} + Y_{PZT} t_{PZT})} \quad (6)$$

Even though this equation is an oversimplification, it provides a useful first approximation of the effect, and it makes three predictions that are confirmed by a more complete analysis.

First, Equation (6) shows that the figure of merit for a PZT material, if the goal is to maximize the Hertz per volt, is $Y_{PZT}\, d_{31}$. If Poisson's ratio had been carried through it would be $Y_{PZT}\, d_{31} / (1-\nu_{PZT})$.

Second, Equation (6) shows that it is best to keep t_{PZT} as small as practical, even if t_{YAG} is fixed, although once $Y_{YAG} t_{YAG} \gg Y_{PZT} t_{PZT}$ there is little value in further reducing t_{PZT}.

Third, it shows that scaling the overall design down while maintaining proportions increases the response per volt as the inverse of the scaling factor.

Table 1 provides relevant values for the parameters of Equation (6).

Table 1: Material properties and dimensions of the µNPRO.

Young's Modulus of YAG, Y_{YAG}	277 GPa
Young's Modulus of PZT material 3265HD, Y_{PZT}	69 GPa
Poisson's ratio of YAG, ν_{YAG}	0.30
Poisson's ratio of PZT material 3265HD, ν_{PZT}	0.32
Charge constant of PZT material 3265HD, d_{31}	-370 picometers/volt
Thickness of YAG for NASA µNPRO, t_{YAG}	1.75 mm
Thickness of PZT for NASA µNPRO, t_{PZT}	0.25 mm
Optical frequency at 1064 nm	282 THz
Optical frequency at 1319 nm	227 THz

For the 1064 nm line of Nd:YAG, the PZT tuning coefficient calculated using Equation (6) is 14.3 MHz/volt. For 1319 nm, it is 11.5 MHz/volt. These values would be increased by about 3.6% if t_{PZT} were reduced to zero. Keeping the $(1-\nu)$ factors increases the calculated response by 1.4%.

3.2 Effect of change in index due to elasto-optic effect

The index of refraction changes with strain, and that also leads to tuning. This effect may increase or decrease the tuning coefficient relative to the result above, depending on both the polarization of the light and the orientation of the crystal. A complete calculation would be quite complex, because in YAG the strength of the elasto-optic effect varies a great deal as crystal orientation changes. This section calculates the effect for two simple cases that give an indication of both the magnitude and the variability of the effect.

The orientation for which the calculation of the elasto-optic effect is easiest is where the <100> crystalline axis and the equivalent <010> and <001> axes are aligned with the major planes defining the NPRO block. For this case a relatively simple equation gives the effect of the index change due to strain relative to the effect that is due to dimensional change alone, that is to say, relative to the value calculated using Equation (6). The equation for light polarized along the y axis (perpendicular to the plane of the PZT/YAG interface, or "vertical") is

$$\frac{index\ effect}{dimensional\ effect} = -\frac{n^2}{2}(-2\,\nu\,p_{11} + 2(1-\nu)\,p_{12})/(1-\nu) \quad (7)$$

where n is the index of refraction of YAG, ν is the Poisson's ratio of YAG, and p_{11} and p_{12} are elements of the elasto-optic tensor[8]. Table 2 has the relevant values. For the values of Table 2, Equation (7) gives a value of -7.13%. The PZT response is reduced due to the elasto-optic effect.

Table 2: Material properties of YAG used to calculate the elasto-optic effect on strain tuning.

Index of refraction of YAG, n	1.82
Poisson's ratio of YAG, ν_{YAG}	0.30
YAG elasto-optic coefficient p_{11}	-0.0290
YAG elasto-optic coefficient p_{12}	0.0091
YAG elasto-optic coefficient p_{44}	-0.0615

For the other polarization, in the plane of the PZT-YAG interface or "horizontal," the corresponding equation is

$$\frac{index\ effect}{dimensional\ effect} = -\frac{n^2}{2}\big((1-\nu)\,p_{11} + 2(1-3\,\nu)\,p_{12}\big)/(1-\nu) \quad (8)$$

For the values of Table 1, Equation (8) gives value of +4.59%. The PZT response is increased.

If the crystalline axes of the YAG are re-oriented such that the axis of propagation remains one of the <100> equivalents, but the other two <100> equivalents are at 45° relative to the plane of the PZT/YAG interface, then the deviation from the "dimensional effect only" case is significantly larger. The equations corresponding to Equations (7) and (8), for this "45° rotated" case, are given below.

The equation for light polarized along the y axis (perpendicular to plane of PZT-YAG interface, vertical) is

$$\frac{index\ effect}{dimensional\ effect} = -\frac{n^2}{4}\big((1-3\nu)\ p_{11} + (3-5\,\nu)\,p_{12} - (2-2\nu)p_{44}\big)/(1-\nu) \quad (9)$$

Equation (9) gives a value of -20.19%.

For the other polarization, in the plane of the PZT-YAG interface, the corresponding equation is

$$\frac{index\ effect}{dimensional\ effect} = -\frac{n^2}{4}\big((1-3\nu)\ p_{11} + (3-5\,\nu)\,p_{12} + (2-2\nu)p_{44}\big)/(1-\nu) \quad (10)$$

Equation (10) gives a value of +17.64%.

Table 3 summarizes these four cases. Other cases have been calculated, and it appears that the two that are tabulated are the "extreme" cases; other orientations seem of fall within the range defined by these two.

It is clear that the YAG elasto-optic effect is highly anisotropic. It is also clear that the effect of the elasto-optic effect, while significant, is much smaller than the effect of dimensional change. Unless there is a need for extreme unit-to-unit consistency, it is not worth the trouble to orient YAG for NPRO manufacturing. Variation from unit to unit in PZT response will be dominated by the challenge of controlling the distance between the resonant laser beam and the PZT/YAG interface.

Table 3. Elasto-optic deviation of total PZT response from the response due to dimensional change only, for two cases with the <100> axis being the axis of beam propagation

YAG Crystal Orientation:	Vertical polarization (along y)	Horizontal polarization (along x)
<010> axis normal to PZT/YAG interface	-7.13%	+4.59%
<010> axis 45° to PZT/YAG interface	-20.19%	+17.64%

The polarization of the internal beam in an NPRO is elliptical, but with most of the power in the "vertical" polarization. In the two cases of Table 3, the elasto-optic effect will reduce the PZT tuning of typical NPROs.

3.3 Two-dimensional numerical calculation of deformation of PZT/YAG composite structure

The simple "two spring" model assumes that strain in the YAG is constant throughout, which is far from the truth. In fact, the strain is concentrated in a region close to the PZT/YAG interface. Locating the laser beam close to this interface will greatly enhance the PZT coefficient.

The exact shape of a NPRO deformed by a PZT element will depend on the details of the NPRO geometry. In order to get a solution that is more general but demonstrates the nature of the distortion, we chose to calculate the distorted shape of an infinitely long piece of YAG with a rectangular cross-section. Referring back to Figure 3, the dimension *x* is infinite.

Calculations with this geometry can be done using the "plane strain" assumption. Under this assumption, all displacement is assumed to be in y-z plane. There are established techniques for numerically solving plane strain problems.[9]

Figure 5 shows cross-sections of three calculated PZT/YAG structures, highly exaggerated in the horizontal direction. All three have the same voltage applied to the PZT. The middle case has the dimensions used in the μNPRO.

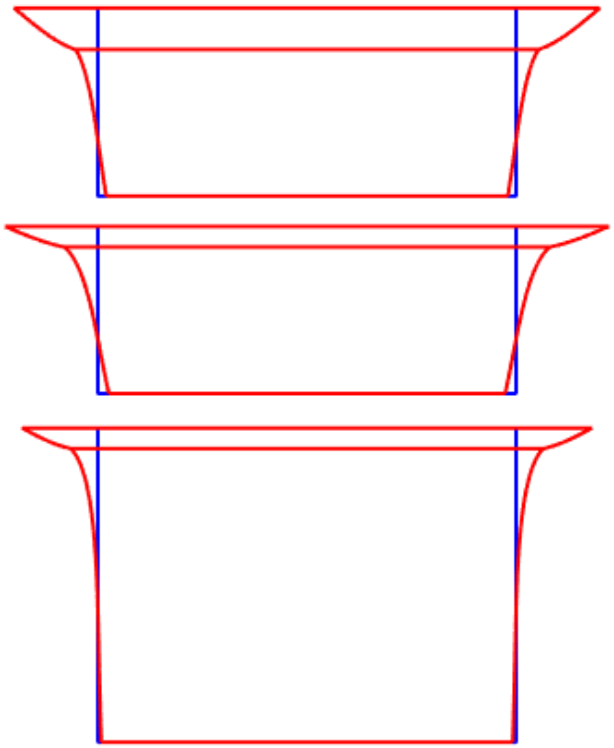

Figure 5. Three PZT/YAG composite structures, with the distorted shape exaggerated in the horizontal dimension only. For all three the voltage applied to the PZT is the same. The middle case is the μNPRO. The top case has a thicker PZT. The bottom case has a thicker NPRO. The blue vertical lines show the undistorted surface.

A noteworthy result is that there is a position in the YAG where there is no displacement. Farther from the PZT/YAG interface the displacement actually changes sign. It is clear that it is desirable to have the laser beam as close as is practical to the PZT/YAG interface.

The top case in Figure 5 shows what happens when the PZT is made thicker, in this case, by a factor of two. With a smaller internal field, the PZT would be expected to strain half as much. But since it is stiffer due to its greater thickness, it can strain the YAG by almost as much as the thin PZT. As in the simple spring model of Equation (6), a thicker PZT will reduce tuning, but not by much once t_{pzt} goes below a small fraction of the YAG dimension.

The third case shows what happens when the thickness of the YAG is doubled. This deformed region remains about the same in absolute size. The deformed region extends downward for a distance of about 25% of the horizontal dimension of the NPRO.

Figure 6 expresses the deformation of the YAG as a tuning coefficient, using Equation (2). For the μNPRO design, three reflection points are at a distance 0.25 mm from the PZT/YAG interface and the fourth is at 1.25 mm. According to Figure 6, the fourth point is in the region where the distortion has the opposite sign. The expected tuning coefficient if all reflections were at a distance of 0.25 mm from the lase plane would be 23.6 MHz/Volt.

It is clear from Figure 6 that the tuning coefficient will be a strong function of the "lase plane" beam position. This will result in unit-to-unit variability in the coefficient if there is inconsistency in the fabrication of the NPROs.

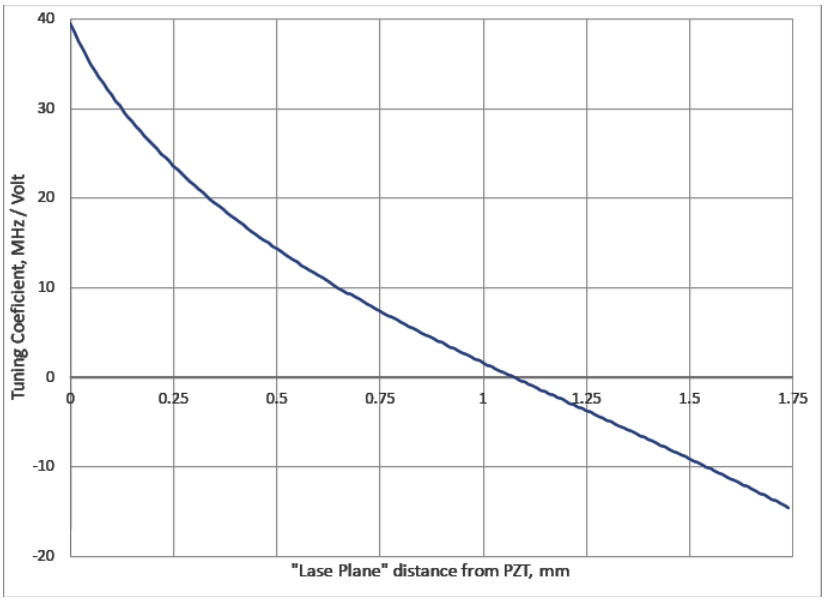

Figure 6. Tuning coefficient calculated as a function of the distance from the PZT/YAG interface to the laser beam, for the μNPRO design dimensions. This calculation ignores the nonplanarity of the NPRO.

Our final estimate of the tuning coefficient was made by assuming that the four μNPRO reflection points move relative their centroid according to Figure 6, with motion determined by the distance from that point to the PZT/YAG interface. This assumption allows the calculation of the change in the round-trip path. The resulting tuning coefficient value is 17.6 MHz/Volt. It will be seen that his estimate is quite close to reality.

3.4 Finite element calculation of first mechanical resonance

A limit on the usefulness of a frequency-tuned oscillator is the speed of response. For piezo-tuning, the response is flat in frequency until the first resonance. We estimated the first resonance using finite element analysis. For a block of YAG of dimensions 5.7 x 4.4 x 1.75 mm, the first resonance was a torsion resonance at 338 kHz. This also will be seen to be close to reality.

If it is desired to increase the useful frequency bandwidth, then the NPRO should be made thicker, at least until the thickness dimension t_{YAG} matches the other two dimensions. This will increase the frequency of the flexural and torsion resonances. Reducing the long dimensions will also increase the resonance frequency.

4. EXPERIMENTAL RESULTS

4.1 Controlling the distance from the PZT/YAG interface to the resonant beam path

Figure 7 shows the design of the µNPRO. It is designed so that the distance from the "lase plane," which is the plane containing the larger of the two isosceles triangles which define the resonant beam path, is 0.25 mm from the PZT/YAG interface. Controlling that dimension accurately requires good tooling. The tooling used to manufacture the µNPRO has all of the angles and dimensions built in, so that the fabrication process is no more difficult than for any other piece of YAG. The cost of producing a µNPRO is driven by the size of the Cr:Nd:YAG starting material and the area of the polished surfaces. The compound angles do not impact the cost once the tooling is designed and produced. The µNPRO is produced in batches of 24.

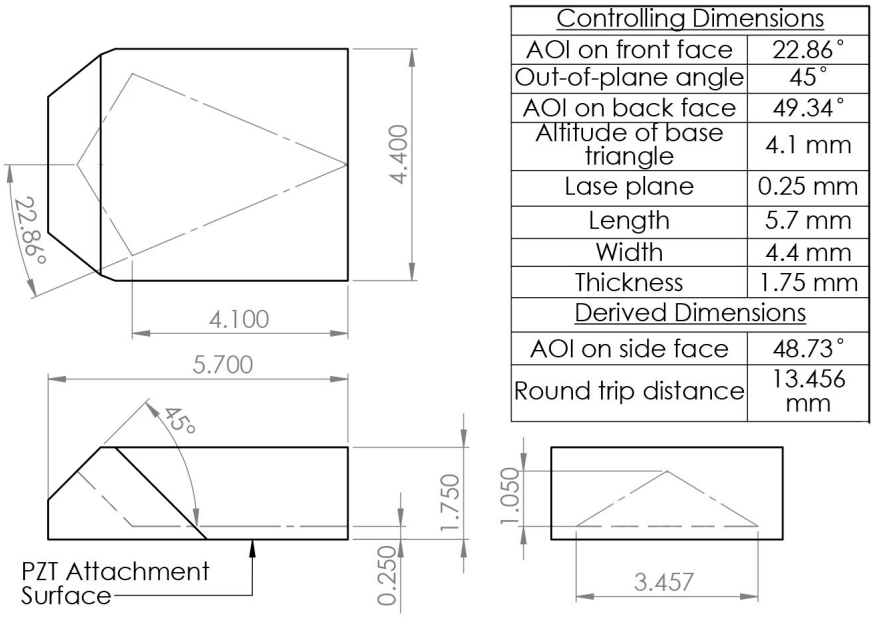

Controlling Dimensions	
AOI on front face	22.86°
Out-of-plane angle	45°
AOI on back face	49.34°
Altitude of base triangle	4.1 mm
Lase plane	0.25 mm
Length	5.7 mm
Width	4.4 mm
Thickness	1.75 mm
Derived Dimensions	
AOI on side face	48.73°
Round trip distance	13.456 mm

Figure 7. Dimensioned drawing of the µNPRO monolithic resonator. The dashed lines are the beam path.

The µNPRO has been produced both with all-planar reflecting surfaces, in which case the beam properties are determined by thermal lensing, and with an *R=150* mm convex curvature on the front face.

An initial concern was the yield of the µNPRO. The position of the resonant ray cannot be adjusted once the µNPRO is manufactured, and if the resonant ray is too close to the edge of the part, or outside the part, then the device will never reach lasing threshold at any amount of pump power. We had parts produced by three manufacturers. All had adequate control of lase plane position. Table 4 shows the statistics of the three manufacturers.

Table 4. Distribution of "Lase Plane" position for µNPROs produced by three fabricators

µNPRO Fabricator	Number tested	Average position of "Lase Plane" (0.25 mm by design)	Standard Deviation of "Lase Plane"
#1	7	0.26 mm	0.02 mm
#2	62	0.20 mm	0.06 mm
#3	4	0.24 mm	0.03 mm

The "Lase Plane" is measured by observing the µNPRO while it is lasing. A camera is positioned so that it can look into the front face of the µNPRO at normal incidence. The view is the same as the lower-right view of Figure 7. Figure 8 shows such a view.

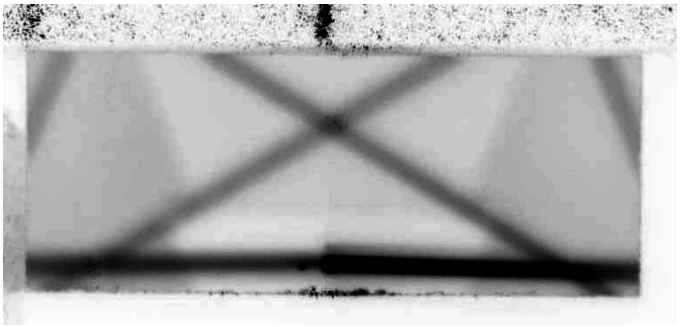

Figure 8. View looking in to the front face of a μNPRO while it is lasing. The beams are dark, since this is a negative image. The central triangle is the beam path. The beams outside the triangle are views reflected by the internal facets of the μNPRO. Photographs such as this allow the measurement of the "lase plane."

4.2 Choice and properties of PZT material

The PZT material that we used has the highest figure of merit $Y_{PZT}\, d_{31}$ that we are aware of. The PZT material chosen is 3265HD available from CTS Corporation[10]. The thickness we used was 0.25 mm. For an 0.25-mm part the maximum recommended voltage is 125 volts. The shape of the PZT closely matches the top surface of the μNPRO, with no overhang, as can be seen in Figure 1. A wrap-around electrode is used. It is important that the PZT element have no overhang. Overhang will create undesirable low-frequency resonances in the response. Table 5 summarizes the properties of the PZT material and the specific part we used.

Table 5. Properties of the PZT material and the specific part we used

Young's Modulus of PZT material* 3265HD, Y_{PZT} or Y^E_{11}	69 GPa
Poisson's ratio of PZT material 3265HD, ν_{PZT}	0.32
Charge constant of PZT material 3265HD, d_{31}	-370 picometers/volt
Thickness of PZT for NASA μNPRO, t_{PZT}	0.25 mm
Area of PZT for NASA μNPRO, A	21 mm^2
Dielectric constant of PZT material 3265HD, K^T_3	6500
Capacitance of PZT, according to $C = K^T_3\, \varepsilon_0\, A / t_{PZT}$	4780 pF

*The Young's Modulus of a PZT depends on both its orientation and on whether it is measured "open circuit" (charge held constant) or "short circuit" (voltage held constant.) The relevant value of Y for our design is designated by PZT manufacturers as Y^E_{11}, the short-circuit elastic constant perpendicular to the poling direction.

The PZT is bonded to the YAG by the epoxy 353-ND. This epoxy has low viscosity right before it cures, so that a very thin bond can be created.

The μNPRO was mounted to its temperature-controlled support using a compliant adhesive, so that the YAG is free to deform, limited only by its own stiffness.

4.3 Measurement of tuning coefficient

Figure 9 shows frequency as a function of time for a PZT-tuned μNPRO driven by a 1-kHz triangle wave with peak-to-peak drive of 192 volts. The peak-to-peak frequency excursion is 3.5 GHz. The tuning coefficient is 3.5 GHz / 192 volts = 18.2 MHz/volt. This is a surprisingly good match to the estimate of 17.6 MHz/volt from section 3.3. For Figure 9, the frequency was measured every 0.4 μsec, so there are 7000 frequency values displayed. The actual data was taken in such a way that the beat frequency never exceeded the 1 GHz limit of our oscilloscope. When the beat note passed through zero and "reflected," the reflected values were inverted, and when it exceeded 1 GHz, the μNPRO temperature was adjusted to bring it back down, and then the data was patched together. Then all values were offset so that the minimum frequency was zero.

We also tested the frequency modulation with a 100 kHz sine wave with a peak-to-peak voltage of 64 volts. The peak-to-peak frequency excursion was 1.03 GHz, indicating a tuning coefficient of 16.1 MHz/volt.

All measurements of frequency were made by observing a beat note with a reference NPRO on an oscilloscope. A digitizing oscilloscope with a long record length (many millions of points) is a very useful tool for frequency analysis. A quasi-sinusoidal record of voltage as a function of time can be converted into frequency as a function of time, and then that record analyzed. Appendix 1 is a snippet of Matlab code that converts a voltage record into a frequency record. It makes use of the "analytic signal[11]."

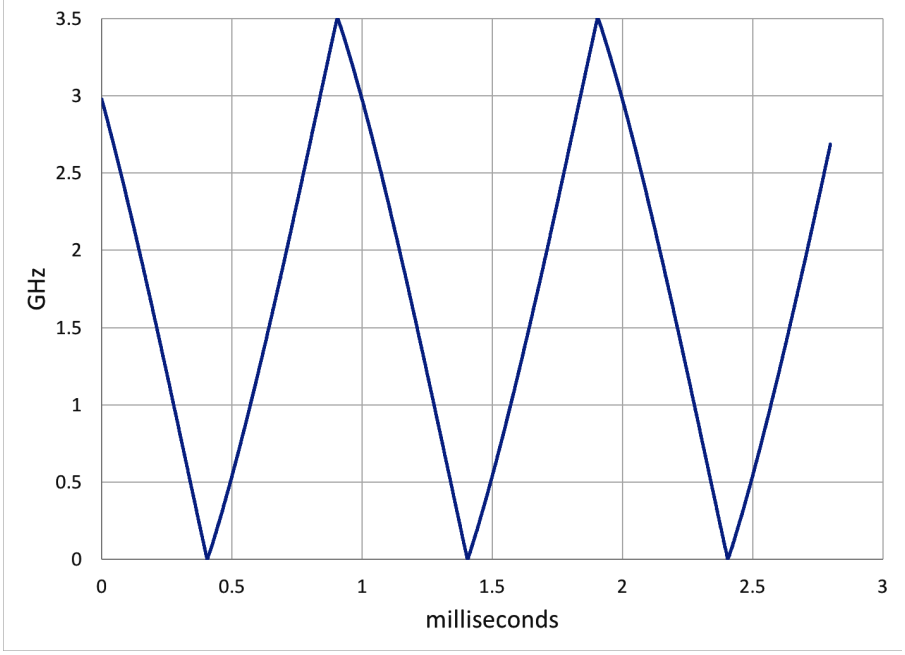

Figure 9. Beat frequency of a μNPRO as a function of time with a 1 kHz triangle wave of amplitude 192 volts peak-peak applied to the PZT. Time resolution is 0.4 μsec, so 7000 points are displayed. No smoothing was applied to the data.

We measured the response of the PZT as a function of Fourier frequency by driving the PZT with white noise of known spectral density, creating the frequency vs. time record, and then calculating its spectral density. This resulted in Figure 10, which shows the response of the PZT from DC to 1 MHz. The first resonance at 323 kHz limits the "flat response" region. This closely matches the theoretical estimate of 338 kHz from section 3.4. Very high response of 206 MHz/volt exists at the 908 kHz resonance. There is an anti-resonance near 420 kHz.

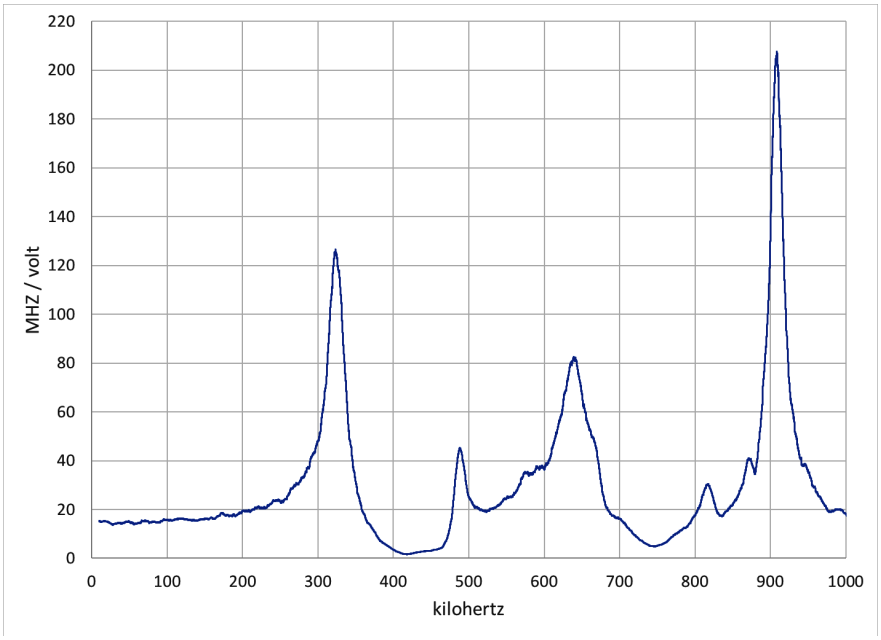

Figure 10. PZT response as a function of frequency. The first resonance at 323 kHz limits the "flat response" region.

5. USEFULNESS FOR FMCW LIDAR

In a typical FMCW LIDAR measurement, the frequency is modulated to create a triangle wave, such as that of Fig 9. Return signal is heterodyned against the outgoing signal. This creates a beat frequency which indicates the distance to the target.

The ideal source for FMCW LIDAR has the following characteristics:

- High power at an eye-safe wavelength.
- Large depth of modulation. This determines the spatial resolution. With modulation depth of 3 GHz, a spatial resolution of a few centimeters is possible.
- Fast modulation with high linearity. This determines the data rate. With a 10 kHz modulation frequency, 10,000 measurements per second can be made with maximum useful range of about 10 km.
- Narrow linewidth.

The NASA μNPRO operates at 1064 nm. At this wavelength enormous power is possible due to amplification, but eye safety is problematic for terrestrial applications. NPROs also operate at 1319 nm, with power about 60% of what is available at 1064 nm, but without the possibility of practical amplification. Commercial NPROs at 1319 nm have power up to 0.5 watts. The 1319 nm wavelength is in the range at which light is the least hazard to the eye, as evidenced by the more permissive Class 1 allowable power. Figure 11 shows the standard.

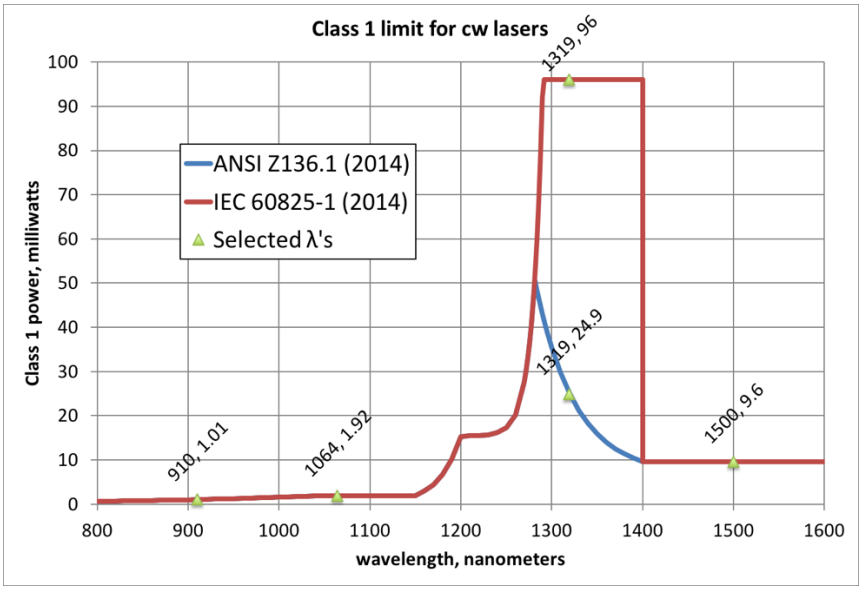

Figure 11. Class 1 "eye-safe" laser power as function of wavelength for a laser with a small, collimated beam. The wavelength range between 1.2 and 1.4 μm is the range of greatest allowable power, because water absorption is enough to protect the retina, while not so much that absorbed power is concentrated right at the surface. The two standards agree at all wavelengths except the range from 1280 nm to 1400 nm. In this range, the ANSI standard is stricter.

The NPRO design results in the narrowest linewidth of any laser type. One way to characterize linewidth is as a power spectral density, in units of Hertz / Hertz$^{1/2}$. Figure 12 plots that performance measure for the μNPRO. It is well-fit by a function that declines as 1/frequency. At 10 kHz the power spectral density of the frequency fluctuation is 1.77 Hertz / Hertz$^{1/2}$. This is a typical value for commercial NPROs. A measurement done in 0.1 msec will have roughly a 10 kHz effective bandwidth so the frequency fluctuation in 0.1 msec is roughly 1.77 Hertz / Hertz$^{1/2}$ • √10 kHz = 177 Hertz. This makes a negligible contribution to the error of the LIDAR measurement.

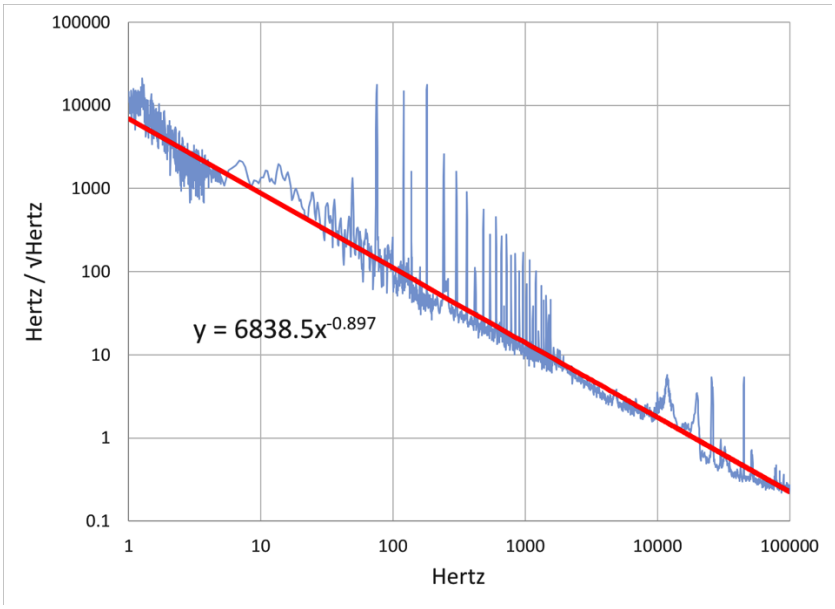

Figure 12. Power spectral density of the frequency fluctuations of a µNPRO. The data has many spikes due to pick-up in the instrumentation. They are not due to the µNPRO. The data fit well to a function with roughly 1/f behavior. At 10 kHz the power spectral density of the frequency fluctuation is 1.77 Hertz / Hertz$^{1/2}$.

6. CONCLUSION

The combination of high power, narrow linewidth, fast, broad tunability and (at 1319 nm) an eye-safe wavelength make the NPRO an attractive option for long-range FMCW LIDAR or other applications where frequency agility is needed. NPROs can be produced in large batches at high yield, and while they will never be the cheapest approach, the cost should not be prohibitive when high performance is needed.

Acknowledgements: The authors acknowledge the financial support of the NASA Physics of the Cosmos Program Office. Thanks to Jim Morehead for help with the elasto-optic tensor calculations.

APPENDIX

Matlab code for converting a quasi-sinusoidal record of voltage into a record of frequency, with one frequency data point for each 2000 voltage data points

```
% The following variables must already exist:
%   dt is delta-t, the time increment between points, units of seconds
%   ts is time series, a long sequence of voltage measurements spaced by dt
ts = ts - mean(ts); % Eliminate any DC term from the data
LL = length(ts);    % Find out how many data points are in ts
m = ceil(LL/2);     % m is the number of Fourier frequencies
q = fft(ts);        % q is the Fourier transform of ts
q(2:m) = 1i * q(2:m);
q(m+1:end) = -1i * q(m+1:end);
if ~mod(LL,2)
    q(m+1) = 0;
end
q = ts – 1i* ifft(q);
% q is now something called the Analytic Signal, a complex function
% Its real part is ts, but its imaginary part is ts “delayed” by 90 degrees
q = unwrap(angle(q));
% Now q is the phase in radians as a function of time, still spaced by dt
q = q(1:2000:end);  %Now the phase values are spaced by 2000*dt
f=0.5*(q(2:end)-q(1:end-1))/dt/2000/pi;
% f is the frequency record, in Hertz, spaced by 2000*dt
```

REFERENCES

[1] Kane, T. and Byer, R. L., "Monolithic, unidirectional single-mode Nd:YAG ring laser," Opt. Lett. 10, 65-67 (1985).
[2] https://resource.lumentum.com/s3fs-public/technical-library-items/npro125126-ds-cl-ae.pdf
[3] https://www.ipgphotonics.com/en/products/lasers/cw-fiber-amplifiers/cw-fiber-amplifiers/yar-lp-sf-1-100-w
[4] Bode N., Briggs J., Chen X., Frede M., Fritschel P., Fyffe M., Gustafson E., Heintze M., King P., Liu J., Oberling J., Savage R.L., Spencer A., Willke B., “Advanced LIGO Laser Systems for O3 and Future Observation Runs” *Galaxies* (2020).
[5] Kane, T., US Patent 4,829,532, “Piezo-electrically tuned optical resonator and laser using same” (1989).
[6] Kane, T. and Cheng, E.A.P., "Fast frequency tuning and phase locking of diode-pumped Nd:YAG ring lasers," Opt. Lett. **13**, 970-972 (1988).
[7] https://sci.esa.int/web/lisa/-/61367-mission-summary
[8] https://www.ctscorp.com/wp-content/uploads/CTS-Piezoelectric-Material-Properties_Full-List_July21.pdf
[9] Timoshenko, S. P. and Goodier, J. N, [Theory of Elasticity], McGraw Hill, (1934) and (1970).
[10] Johnson, V. R. and Olson F. A, "Photoelastic properties of YAG," Proceedings of the IEEE, vol. 55, no. 5, pp. 709-710, (1967),
[11] Bracewell, R. N., [The Fourier Transform and its Applications], McGraw Hill, 267-272 (1978).